

1
2
3
4
5
6
7
8 Multi-Color Emitting Block Copolymer-Integrated Graphene Quantum
9
10 Dots for Colorimetric, Simultaneous Sensing of Temperature, pH, and
11
12
13 Metal Ions
14
15

16
17
18 *Chan Ho Park,¹ Hyunseung Yang,¹ Junhyuk Lee,¹ Han-Hee Cho,¹ Dahin Kim,¹ Doh C. Lee,*
19
20 *¹ Bumjoon J. Kim^{*,1}*
21

22
23 ¹Department of Chemical and Biomolecular Engineering, Korea Advanced Institute of Science
24
25 and Technology (KAIST), Daejeon 305-701, Korea
26
27
28
29
30

31
32 **Keywords**

33
34 colorimetric sensor, multi-functional sensor, graphene quantum dots, stimuli-responsive
35
36 polymer, block copolymer
37
38
39
40
41
42
43
44
45
46
47
48
49
50
51
52
53
54
55
56
57
58
59
60

1
2
3
4
5
6
7
8
9
10
11
12
13
14
15
16
17
18
19
20
21
22
23
24
25
26
27
28
29
30
31
32
33
34
35
36
37
38
39
40
41
42
43
44
45
46
47
48
49
50
51
52
53
54
55
56
57
58
59
60

ABSTRACT

Highly-selective optical sensors that are capable of detecting complex stimuli have attracted significant interest in environmental, biomedical, and analytical chemistry applications. In this work, we report the development of novel and versatile platform for highly-efficient, colorimetric multi-functional sensors using block copolymer-integrated graphene quantum dots (bcp-GQDs). In particular, the multi-functional sensing behavior is successfully generated simply by grafting blue emitting, temperature-responsive block copolymers onto green-emitting, 10-nm size GQD with the GQD providing luminescent response to pH changes. Thus, the bcp-GQDs showed simultaneous, orthogonal sensing behavior to temperature and pH, as well as dose-dependent responses to different types of metal ions. In addition, the bcp-GQD sensor showed excellent reversibility and dispersion stability in pure water, indicating that our system is an ideal platform for environmental and biological applications. The detailed mechanism of the responsive behavior of the bcp-GQDs was elucidated by measurements of time-resolved fluorescence and dynamic light scattering.

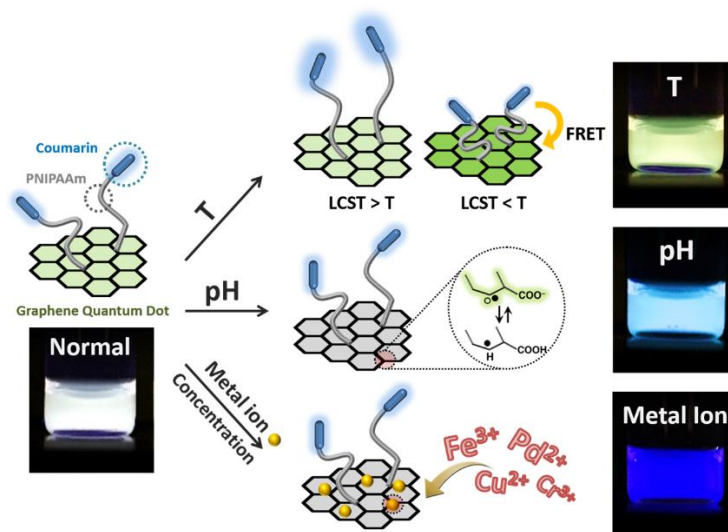
1
2
3
4 INTRODUCTION
5

6
7 Fluorescent materials have attracted significant attention for a wide variety of applications,
8
9 ranging from optoelectronic devices to chemical and biological sensors.¹⁻⁴ Particularly,
10
11 fluorescent multi-functional sensors, which respond simultaneously and independently to
12
13 different stimuli, have been the center of research interest due to their simple detection of
14
15 multiple stimuli in a complex environment.⁴⁻⁶ These multi-functional sensing behaviors are
16
17 typically achieved by integrating different responsive objects, such as stimuli-responsive small
18
19 molecules, polymers, and/or inorganic particles into a single platform.^{6, 7} However, such
20
21 sensors typically require a multistep and complex synthesis of different types of responsive
22
23 components.^{8,9} Additionally, many functional sensors based on small molecules and polymers
24
25 often suffer from poor dispersion in aqueous media and toxicity, which limit their use in
26
27 biological and environmental applications.¹⁰⁻¹² More importantly, most fluorescent sensors
28
29 respond to stimuli by a single photoluminescence (PL) intensity change that often requires an
30
31 expensive PL detector to monitor the response effectively.¹³⁻¹⁵
32
33
34
35
36

37
38 Graphene quantum dots (GQDs), nanometer-sized graphene derivatives, have very
39
40 interesting opto-electronic properties due to quantum confinement and edge effects.¹⁶⁻²¹
41
42 Therefore, in contrast to graphene and graphene oxide that do not exhibit strong stimuli-
43
44 responsive or luminescent behaviors, GQDs have tunable luminescent properties that depend
45
46 on their size as well as pH and the presence of metal ions, making them great candidates for a
47
48 multi-sensing platform.^{18, 22-28} In addition, their surface typically has functional, oxygen-
49
50 containing groups that provide excellent water-solubility as well as reactive sites for surface
51
52 modification.¹⁹ Despite such advantages, the multi-sensing behavior of GQD-based materials
53
54 has not been extensively investigated.^{29, 30} To the best of our knowledge, the colorimetric,
55
56 multi-sensing response of the GQD-based sensors has not been demonstrated despite its great
57
58 advantage of rapidly readable responses.
59
60

1
2
3
4
5
6
7
8
9
10
11
12
13
14
15
16
17
18
19
20
21
22
23
24
25
26
27
28
29
30
31
32
33
34
35
36
37
38
39
40
41
42
43
44
45
46
47
48
49
50
51
52
53
54
55
56
57
58
59
60

Herein, we describe the development of a colorimetric, multi-sensing platform based on responsive block copolymer-integrated GQDs (bcp-GQDs) that detect different types of information simultaneously, including temperature, pH, and various kinds of metal ions. Our synthetic approach is very simple, involving single-type blue emitting, thermally-responsive poly(7-(4-(acryloyloxy)butoxy)coumarin)-*b*-poly(N-isopropylacrylamide) (P7AC-*b*-PNIPAAm) polymers grafted to green-emitting, 10-nm GQDs (**Scheme 1**). A key strategy for generating colorimetric, multi-sensing behavior is to control the relative amounts of blue emission from P7AC-*b*-PNIPAAm and green emission from the GQD core, which are both strongly dependent on different types of stimuli. The colorimetric sensing response to temperature change was generated by tuning the distance between the blue and green emitters and, thus, their Förster resonance energy transfer (FRET). In addition, the luminescent response of the green-emitting GQD core produced quantitative, colorimetric switching behavior of bcp-GQDs in response to changes in pH and different types of metal ions. The detailed mechanism of the responsive behavior of the bcp-GQD sensors was investigated using time-resolved photoluminescence spectroscopy, dynamic light scattering, and microscopy. To the best of our knowledge, this is the first colorimetric, multi-functional sensor based on GQDs.



Scheme 1. Structure of block copolymer-grafted graphene quantum dots (bcp-GQDs) and their sensing behavior.

RESULTS AND DISCUSSION

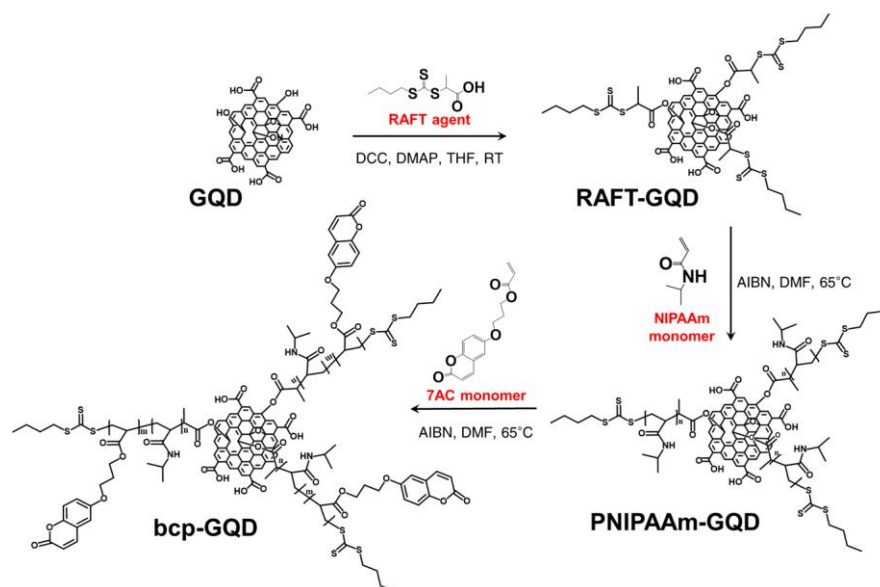


Figure 1. Synthesis of bcp-GQDs

Figure 1 shows the synthetic procedure employed to produce fluorescent P7AC-*b*-PNIPAAm block copolymer-grafted GQDs. Green-emitting GQDs were synthesized by the cleavage of carbon black (CX-72), as reported in a previous study.^{25, 26} Blue-emitting P7AC-*b*-PNIPAAm diblock copolymers were synthesized on the surface of the GQDs by the “grafting-from” method using reversible addition–fragmentation chain transfer (RAFT) polymerization.³¹ First, the trithiocarbonate RAFT chain transfer agent was grafted covalently onto the surface of the pristine GQDs by the *N,N'*-dicyclohexylcarbodiimide (DCC) coupling reaction between the hydroxyl group on the GQD surface and the carboxylic acid group of the RAFT agent.^{11, 32} The functionalized GQDs were then precipitated, centrifuged, and filtered several times to remove ungrafted RAFT agent and other chemical residues completely, which was confirmed using thin-layer chromatography. For convenience, RAFT chain transfer agent-grafted GQDs are denoted as RAFT-GQDs. The PNIPAAm block was polymerized from the RAFT-GQDs, followed by the blue emitting P7AC block to produce P7AC-*b*-PNIPAAm block

1
2
3
4 copolymer chains on the GQDs (bcp-GQDs). Since the molecular weight (M_n) of the
5
6 PNIPAAm block is a critical parameter that determines the distance between the two
7
8 chromophores and the M_n of the P7AC block influences the brightness of the blue emitters, the
9
10 M_n of both the PNIPAAm and P7AC blocks were controlled carefully.¹³ The total M_n of P7AC-
11
12 *b*-PNIPAAm of bcp-GQD was 6.4 kg mol^{-1} with a polydispersity index (PDI) of 1.16. The M_n
13
14 and PDI values of the PNIPAAm block only were 5.9 kg mol^{-1} and 1.13, respectively. The
15
16 areal chain density (δ) of the grafted P7AC-*b*-PNIPAAm polymers on the GQDs was estimated
17
18 to be $0.035 \text{ chain nm}^{-2}$. The δ value was calculated based on the average size of the GQDs
19
20 using transmission electron microscopy (TEM) images, and the weight fractions of the GQD
21
22 cores and the grafted polymers obtained by thermogravimetric analysis (TGA) (Supporting
23
24 Information (SI) Figure S1).³³⁻³⁵ The δ value is comparable to the values reported previously
25
26 for other systems involving PNIPAAm brushes on graphene.^{13, 36}
27
28
29
30
31
32

33 The conjugation of the P7AC-*b*-PNIPAAm polymers to the surface of the GQDs was
34
35 confirmed by attenuated total-reflectance Fourier transform infrared spectroscopy (ATR-FTIR)
36
37 and X-ray photoelectron spectroscopy (XPS) measurements. As shown in Figure S2a, ATR-
38
39 FTIR of RAFT-GQDs showed stretching vibrations of the thiocarbonyl group (C=S) at 1072
40
41 cm^{-1} , corresponding to the RAFT agent.^{37, 38} The amide peaks from the PNIPAAm blocks in
42
43 the PNIPAAm-GQDs and bcp-GQDs were observed at 1530 , 1640 and 3290 cm^{-1} .³⁸ Compared
44
45 to the PNIPAAm-GQDs, the bcp-GQDs exhibited a slightly increased intensity of the C=O
46
47 stretching peak at 1722 cm^{-1} and a decreased intensity of the amide peak due to the additional
48
49 C=O groups from the P7AC block (SI Figure S2b). In addition, XPS of the functionalized
50
51 GQDs revealed sulfur (S 2p) peak corresponding to the grafted RAFT agent, whereas XPS of
52
53 pristine GQDs did not show any signal (SI Figure S2c). The S 2p peak intensity decreased
54
55 significantly for the PNIPAAm-GQDs and for the bcp-GQDs, because the portion of sulfur
56
57 was diluted by the grafted block copolymers.
58
59
60

We examined the solubility and stability of the bcp-GQDs (SI Figure S3). It was observed that all of the pristine GQDs, RAFT-GQDs, PNIPAAm-GQDs, and bcp-GQDs were dispersed successfully in water. As shown in Figure S3, the green emission of the pristine-GQDs, RAFT-GQDs, and PNIPAAm-GQDs was evident. In stark contrast, the bcp-GQDs showed near white emission due to the simultaneous blue emission of the P7AC block and green emission of the GQDs, demonstrating the potential of bcp-GQDs as luminescent sensors that have tunable fluorescence properties (SI Figure S4). To further confirm the chemical grafting of the block copolymers on the GQDs, the average sizes and heights of pristine GQDs, RAFT-GQDs, and bcp-GQDs were measured and compared by high-resolution TEM and atomic force microscopy (AFM) (SI Figure S5). The average size and height of the GQDs were 11.1 and 0.71 nm, respectively, while the average size and height of the RAFT-GQDs were 11.8 and 0.73 nm, respectively. In contrast, the average size and height of the bcp-GQDs increased significantly to 26.6 and 3.88 nm, respectively, due to the presence of the grafted polymer chains on the GQD surface. These results indicated that the P7AC-*b*-PNIPAAm chains were successfully grafted from the RAFT agent covalently attached to the surface of the GQDs.

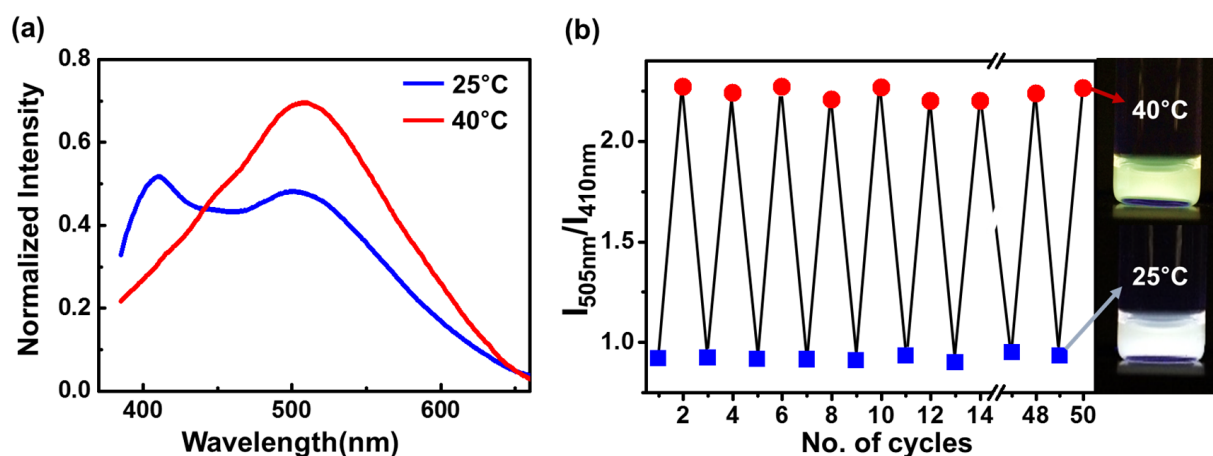


Figure 2. (a) PL spectra of the bcp-GQDs; (b) Reversibility test of the PL behavior of bcp-GQDs with the excitation at 365 nm.

1
2
3
4
5
6
7 Figure 2a shows the PL response of the bcp-GQDs in water (pH 7) as a function of
8
9 temperature. The concentration of the bcp-GQDs was maintained at the low concentration of
10
11 30 ppm to avoid any PL quenching of the P7AC block by other GQD substrates in the solution.
12
13 At room temperature, the PL spectra of the bcp-GQDs showed two emission peaks, one at 410
14
15 nm from the P7AC block and one at 505 nm from the GQD cores, producing near white
16
17 luminescence. When the temperature of the solution increased to 40 °C, the intensity of the
18
19 blue emission peak at 410 nm decreased suddenly, whereas the intensity at 505 nm increased
20
21 significantly, showing green color. To quantify the change in PL intensity in terms of
22
23 temperature and to examine the reversibility of the response behavior of the bcp-GQDs, the PL
24
25 intensity ratios at emission levels of 505 and 410 nm ($I_{505\text{nm}}/I_{410\text{nm}}$) were plotted with
26
27 continuous cycles in aqueous media at different temperatures in Figure 2b. When the
28
29 temperature was increased from 25 to 40 °C, the $I_{505\text{nm}}/I_{410\text{nm}}$ value significantly increased from
30
31 0.91 to 2.27. This change was reproducible over continuous heating-cooling cycles. We
32
33 attribute the extraordinary reversibility and stability of the bcp-GQDs to the strong covalent
34
35 linkage between the grafted polymers and the GQDs, and to the excellent dispersion behavior
36
37 of the GQD substrates in water. Fast response, high reversibility, stability, and visible color
38
39 change are crucial for successful application and commercialization of optical sensors.^{8, 39, 40}
40
41 The colorimetric response of the bcp-GQD solution as a function of temperature was correlated
42
43 with the change in the conformation of the PNIPAAm chain at the lower critical solution
44
45 temperature (LCST). Below 32 °C, the PNIPAAm chains in the bcp-GQDs become hydrophilic
46
47 and stretched in water. Thus, the distance between the two fluorescent units, i.e., the blue-
48
49 emitting P7AC block and the green emitting GQDs, should be long enough to suppress the
50
51 FRET between them. Above the LCST, the PNIPAAm chains collapse, promoting FRET from
52
53
54
55
56
57
58
59
60

the higher energy P7ACs to the lower energy GQDs and producing a color change from white to green.⁴¹⁻⁴³

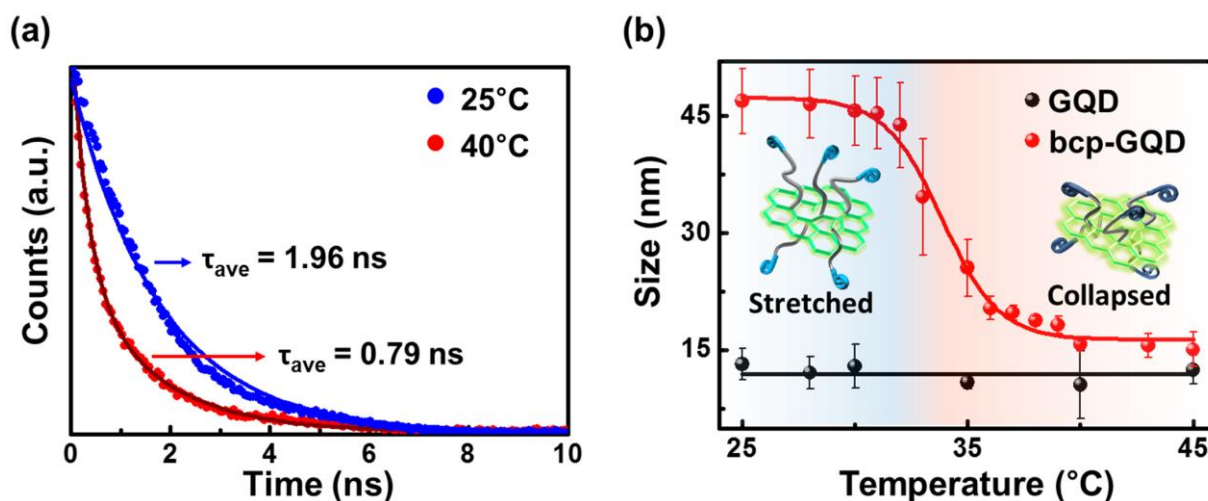


Figure 3. (a) Reversible behavior of the fluorescence decay of bcp-GQDs between 25 °C and 40 °C. Both measurements were performed at 410 nm emission with the excitation at 370 nm. (b) DLS analysis for the sizes of pristine GQDs and bcp-GQDs as a function of temperature.

The FRET efficiency was evaluated by measuring the lifetime of the fluorophores (Figure 3a).⁴⁴⁻⁴⁶ The decay in the fluorescence intensity of the P7AC emission from the bcp-GQDs at 410 nm was investigated by time-resolved fluorescence (TRF) under irradiation at 370 nm in water.⁴⁷ The TRF results indicated that the bcp-GQDs were temperature-sensitive and their fluorescent lifetime decreased significantly at the temperature above the LCST. These results are summarized in Table S1, and the data were fitted using a double-exponential decay model. At 25 °C, below the LCST of the PNIPAAm spacer, the P7AC emission in the bcp-GQDs had an average lifetime (τ_{ave}) of 1.96 ns, with two decay components of $\tau_1 = 1.73$ ns (population $A_1 = 96.34\%$) and $\tau_2 = 7.91$ ns (population $A_2 = 3.66\%$). In contrast, at 40 °C, above the LCST of PNIPAAm, the P7AC emission decay process was much faster, with a τ_{ave} value of 0.79 ns, with decay components of $\tau_1 = 0.52$ ns (population $A_1 = 83.87\%$) and $\tau_2 = 2.19$ ns (population $A_2 = 16.13\%$). The shorter lifetime of the P7AC emission in the bcp-GQDs was attributed to an increase in the non-radiative decay rate caused by energy transfer from the P7ACs to the

1
2
3
4 GQDs. A similar TRF trend after multiple cycles was obtained repeatedly and is consistent
5
6 with that of the reversibility test of the static PL spectra (SI Figure S6).
7
8

9
10 A deeper insight into the dramatic color responses as a function of temperature was
11
12 obtained by examining the change in the size of the bcp-GQDs via dynamic light scattering
13
14 (DLS) (Figure 3b). Pristine GQDs had a temperature-independent, hydrodynamic diameter of
15
16 12 nm, which is in excellent agreement with the size of the GQDs measured by high resolution
17
18 TEM. In stark contrast, the particle sizes of the bcp-GQDs were strongly dependent on
19
20 temperature due to the conformational change of the polymer chains on the GQDs. The particle
21
22 size was constant at 16 nm above the LCST, showing good agreement with the sum of the GQD
23
24 core (~12 nm) and twice the radius of gyration of the PNIPAAm chains (~1.1 nm).^{48, 49} Under
25
26 these temperature conditions, the distance between the P7AC block and GQD core was short
27
28 enough to induce strong FRET from P7AC to the GQD as evidenced by the strong green
29
30 luminescence of the bcp-GQDs. When the temperature was below the LCST, the
31
32 hydrodynamic particle size of the bcp-GQDs was remarkably increased to 45 nm. Under these
33
34 conditions, the distance between the P7AC block and GQD core became significantly larger
35
36 and suppressed the FRET. Because the hydrodynamic particle size can be overestimated by
37
38 DLS measurements due to extensive swelling of the polymers by the solvent,¹¹ the increase in
39
40 the particle size is not equal to the increase in the donor-to-acceptor distance. However, it is
41
42 worthwhile to note that the trend of the particle size dependence on the temperature change
43
44 was consistent with that of the PNIPAAm conformation and the PL spectra in Figure 2. These
45
46 observations described that the dramatic temperature-dependent color response of the bcp-
47
48 GQDs was induced solely by the FRET effect from the P7AC block to the GQD due to the
49
50 changes of PNIPAAm's conformation in response to temperature.
51
52
53
54
55
56
57
58
59
60

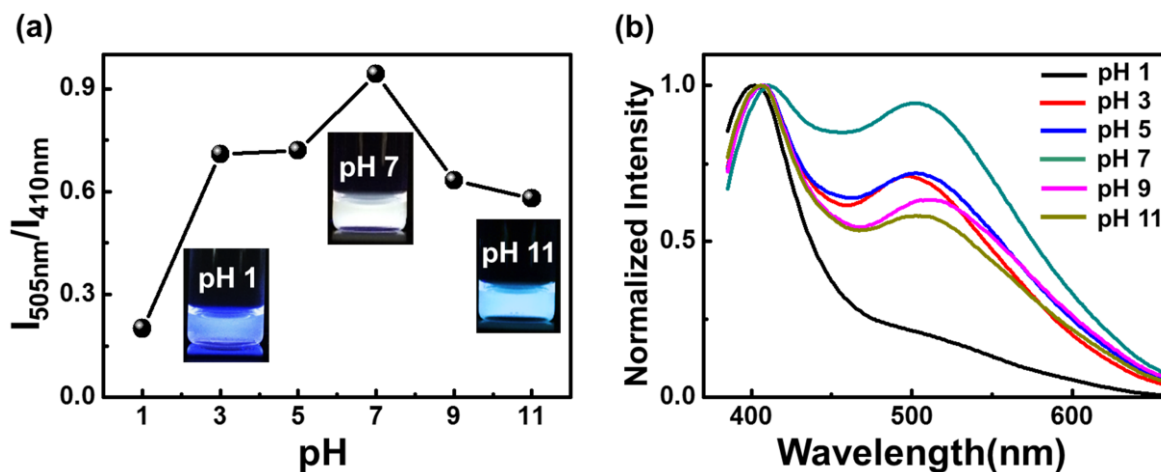


Figure 4. (a) The ratio of PL intensity of bcp-GQDs at different pH values; (b) PL spectra of bcp-GQDs at different pH values from pH 1 to 11 at 25 °C.

To demonstrate the use of the bcp-GQD sensor as a multi-sensing platform, the colorimetric responses of the bcp-GQDs to changes in pH and ion stimuli were investigated. Figure 4 shows the pH-dependent PL behavior of the bcp-GQDs. The color of the solution distinctly turned from blue (pH 1) to white (pH 7) to cyan (pH 11) as the pH increased. For example, the $I_{505\text{nm}}/I_{410\text{nm}}$ value was 0.20 at pH 1, but it increased to 0.71 at pH 3. At pH 7, $I_{505\text{nm}}/I_{410\text{nm}}$ value was highest as 0.94. This is because the emission of the GQD core at 505 nm in the bcp-GQDs decreased as the solution became more acidic. For the same reason, lower $I_{505\text{nm}}/I_{410\text{nm}}$ values were provided as 0.63 at pH 9 and 0.59 at pH 11 than at the neutral condition. Whereas the PL intensity of the bcp-GQDs at 410 nm remained almost constant irrespective of pH change, the emission intensity of the GQDs in strong acidic and alkaline conditions decreased considerably because the pH change can induce protonation or deprotonation of emissive sites (i.e., oxygen groups and free zigzag sites) in the GQD cores.^{18, 26, 50} Thus, the relative amounts of green to blue emissions were tuned in terms of pH value, generating colorimetric behavior. Compared with traditional pH responsive polymer-based sensors that change their conformation only at a specific pH value, our bcp-GQDs system has advantages in monitoring a wide range of pH

values with visible color changes.³⁹ Also, we highlight that simultaneous, orthogonal sensing of changes in temperature and pH can be achieved using our bcp-GQDs (SI Figure S7). The PL and color changes of bcp-GQDs in different pH conditions (i.e., pH 1-11) were observed in terms of temperature change.

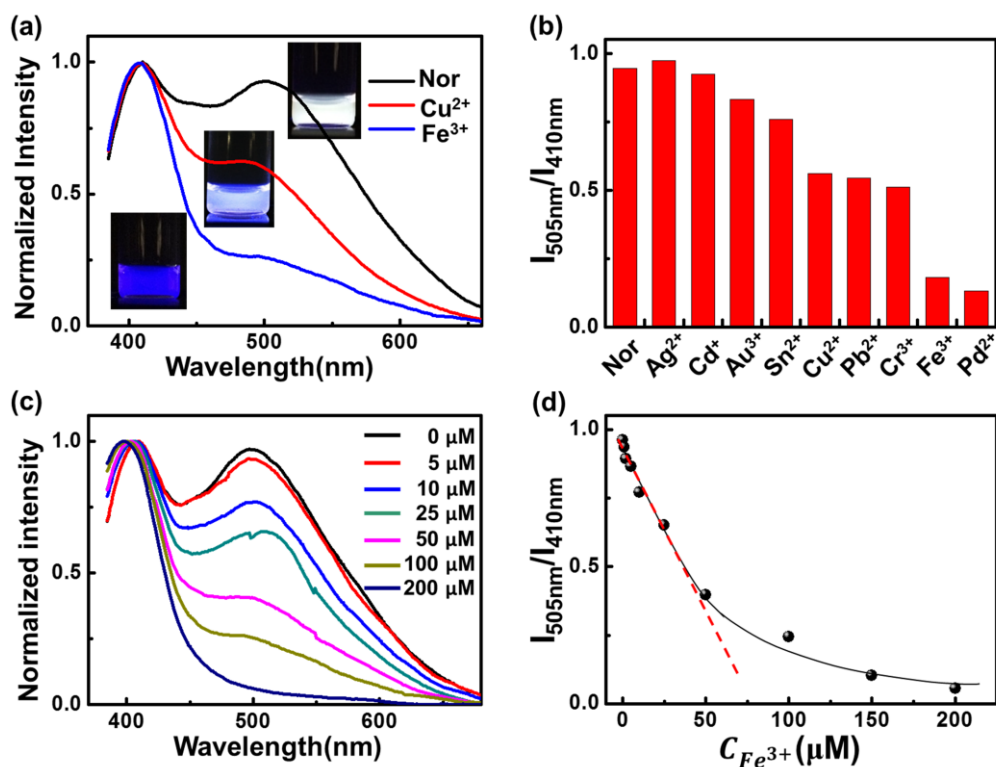


Figure 5. (a) PL spectra of bcp-GQDs at the presence of Cu^{2+} and Fe^{3+} at a concentration of $100 \mu\text{M}$; (b) Ratio of PL intensity upon the addition of $100 \mu\text{M}$ of guest metal ions (Ag^{2+} , Cd^{2+} , Au^{3+} , Sn^{2+} , Cu^{2+} , Pb^{2+} , Cr^{3+} , Fe^{3+} , and Pd^{2+}); (c) PL spectra of bcp-GQDs as a function of the Fe^{3+} concentration (μM); (d) Plot of $I_{505\text{nm}}/I_{410\text{nm}}$ of bcp-GQDs as a function of the Fe^{3+} concentration (The line is a guide for the eye. The PL spectra were measured under irradiation at 365 nm.)

Of particular interest is that the bcp-GQDs can detect various types of metal ions in a dose-dependent manner. Figure 5 highlighted that the bcp-GQD system can be applied for the sensitive detection of metal ions with dose-dependent color distinction. All experiments were performed in pH 7 aqueous solution at $25 \text{ }^\circ\text{C}$. Figure 5a shows changes in the PL spectra of

1
2
3
4 bcp-GQDs in response to Cu^{2+} and Fe^{3+} . The solution of bcp-GQDs turned from white to a
5
6 greenish blue color in the presence of Cu^{2+} at the concentration of 100 μM , whereas the solution
7
8 changed to deep-blue color in the presence of Fe^{3+} at the same concentration. These phenomena
9
10 were caused by the PL response of the GQD core at 505 nm in the presence of different metal
11
12 ions. In this regard, we investigated the color response of the bcp-GQD sensor in the presence
13
14 of various types of metal ions (i.e., Ag^{2+} , Cd^+ , Au^{3+} , Sn^{2+} , Cu^{2+} , Pb^{2+} , Cr^{3+} , Fe^{3+} , and Pd^{2+})
15
16 (Figure 5b). The concentration of the metal ions in the solution was fixed at 100 μM . It was
17
18 observed that the degree of reduction in the green emission of GQD cores relies on the type of
19
20 metal ions, which makes multi-color recognition of bcp-GQDs dependent on the type of metal
21
22 ion. Furthermore, the concentration of the metal ions determines the colorimetric response of
23
24 the bcp-GQDs. For example, we examined the effect of Fe^{3+} concentration on the PL intensity
25
26 of the bcp-GQD cores at 505 nm, which showed a gradual decrease in the intensity as the Fe^{3+}
27
28 concentration increased (Figure 5c). The $I_{505\text{nm}}/I_{410\text{nm}}$ value decreased linearly with respect to
29
30 Fe^{3+} concentration in a range from 0 to 50 μM , enabling the quantitative measurement of the
31
32 Fe^{3+} concentrations (Figure 5d). These results can be explained by the formation of non-
33
34 radiative metal-GQD complexes by the interaction between the GQDs and electrophilic metal
35
36 ions, which contributes to additional fluorescence quenching by charge transfer from the
37
38 excited GQDs to the metal ions.⁵¹⁻⁵⁵ For example, Figure S8 shows that the fluorescence decay
39
40 of GQD cores in bcp-GQDs became much faster in the presence of the 100 μM concentration
41
42 of Fe^{3+} .⁵⁶ Since the degree of formation of metal-GQD complexes is highly dependent on the
43
44 concentration of metal ions and the binding affinity between metal ions and GQDs,⁵⁷ the bcp-
45
46 GQDs showed distinct color responses depending on the concentration and also had different
47
48 PL responses for different metal ions (Figure 5b). In addition, the ion sensing behavior of bcp-
49
50 GQDs was investigated in the presence of different stimuli of temperature and pH. Figure S9
51
52 demonstrates that the bcp-GQDs had simultaneous sensing behavior for temperature and pH,
53
54
55
56
57
58
59
60

1
2
3
4 and they also showed responses to different types of metal ions with excellent stability. The
5
6 colorimetric, orthogonal response of bcp-GQD sensors towards various stimuli sensing is
7
8 potentially advantageous for their use in environmental sensing applications, including tap-
9
10 water analysis, cell diagnosis and bio-imaging.
11
12

13 14 15 16 CONCLUSIONS

17
18 In summary, we developed a novel colorimetric multi-functional sensor using block
19
20 copolymer-integrated GQDs through the “grafting from” method. The bcp-GQDs had
21
22 simultaneous, orthogonal sensing behavior to temperature and pH, as well as dose-dependent
23
24 responses to different types of metal ions with excellent reversibility and stability. All of the
25
26 responses can be easily detected by their distinctive colorimetric changes. Our GQD-based
27
28 sensing platform can be applied easily in various sensor systems with alternate grafted
29
30 molecules, thus providing promising opportunities for use in opto-electronic, environmental,
31
32 and biological applications.
33
34
35
36
37
38
39

40 METHODS

41
42 *Materials:* Vulcan CX-72 carbon black was purchased from Cabot Corporation. Anhydrous
43
44 potassium carbonate (K_2CO_3 , 99.5%), magnesium sulfate ($MgSO_4$, 99%), sodium hydroxide
45
46 (NaOH powder, 98%), and hydrochloric acid (HCl, 10 M) were purchased from Daejung
47
48 Chemical & Metal Co. Azobisisobutyronitrile (AIBN, 98%) was purchased from Junsei
49
50 Chemical Co. and purified by recrystallization from ethanol. 7-hydroxycoumarin and other
51
52 materials were purchased from Sigma-Aldrich and N-isopropylacrylamide (NIPAM, 99%)
53
54 purified by recrystallization in hexane. Deionized (DI) water was used in all experiments.
55
56
57

58
59 *Synthesis of 7-(4-(acryloyloxy)butoxy)coumarin (7AC):* The 7AC monomer was synthesized
60
as previously reported.^{13, 58} Anhydrous K_2CO_3 (3.48 g, 24.8 mmol) was added into a mixture
of 7-hydroxycoumarin (2 g, 12.4 mmol) and 1,4-dibromobutane (4.42 mL, 37.2 mmol) in

1
2
3
4 acetone (120 mL). The resulting suspension was refluxed for 24 h. The precipitate was filtered
5 off, and the solvent was removed. The resulting mixture was diluted with diethyl ether and the
6 separated organic layer was washed with DI water, dried over MgSO₄, and concentrated under
7 reduced pressure. The residue was purified by means of column chromatography using silica
8 gel and a mixture of hexane and ethyl acetate as the eluent, affording 7-(4-bromobutoxy)-
9 coumarin. Then, 7-(4-bromobutoxy)-coumarin (2.38 g, 9 mmol) and excess sodium acrylate
10 (1.128 g, 12 mmol) were dissolved in ethanol (150 mL). Hydroquinone (0.02 g, 1.8 mmol) was
11 added, and the solution was refluxed for 36 h. The precipitate was filtered off and washed with
12 ethanol. After the solvent was removed under reduced pressure, DI water was added, and the
13 residue was extracted with diethyl ether. The residue was purified by column chromatography
14 on silica gel with a mixture of hexane and ethyl acetate as the eluent to yield 7AC (1.4 g, 61%)
15 as a white solid.
16
17

18
19
20
21
22
23
24
25
26
27
28
29
30
31
32
33
34
35
36
37
38
39
40
41
42
43
44
45
46
47
48
49
50
51
52
53
54
55
56
57
58
59
60
¹H NMR (CDCl₃): 7.62 (d, 1H), 7.34 (d, 1H), 6.80 (m, 2H), 6.41 (d, 1H), 6.24 (m, 1H), 6.11
(m, 1H), 5.81 (m, 1H), 4.23 (s, 2H), 4.04 (s, 2H), 1.90 (s, 2H), 1.55 (s, 2H).

33
34
35
36
37
38
39
40
41
42
43
44
45
46
47
48
49
50
51
52
53
54
55
56
57
58
59
60
Synthesis of trithiocarbonate RAFT chain transfer agent: We synthesized (2-(((butylsulfanyl)-
carbonothioyl)sulfanyl))propanoic acid using a procedure modified from previous reports.^{11, 59}
An aqueous solution of NaOH (50 %, 16.0 g) was added to a mixture of butanethiol (18.0 g,
200 mmol) and DI water (30 mL), followed by the addition of acetone (10 mL) to give a
colorless solution. The solution was stirred at room temperature for 0.5 h. Carbon disulfide (14
mL, 17.6 g, 231 mmol) was added to obtain a clear orange solution. The reaction mixture was
stirred for 0.5 h and then cooled in an ice bath. Then, 2-bromopropionic acid (31.4 g, 205 mmol)
was added dropwise, followed by the addition of NaOH_(aq) (50 %, 16.0 g) at a rate such that
the temperature of the bath was kept lower than 30 °C. After the exothermic reaction had
terminated, DI water (30 mL) was added, and the reaction mixture was stirred at room
temperature for 24 h. The reaction mixture was diluted with 50 mL of water. Then, 10 M HCl_(aq)
(60 mL) was added to the solution under an ice bath. A yellow oil was obtained, and kept in an
ice bath until the oil solidified. The solid was separated by filtration, washed with cold water,
and dried. Finally, the product was recrystallized from hexane with gentle stirring to give
bright-yellow solid crystals (34.8g, 71.2%).

¹H NMR (CDCl₃, 500 MHz) δ 9.9 (br s, 1H), 4.87 (q, 1H), 3.37 (t, 2H), 1.66-1.76 (m, 2H),

1
2
3
4 1.64 (d, 3H), 1.42-1.49 (m, 2H), 0.94 (t, 3H).
5
6
7

8
9
10 *Synthesis of GQDs:* GQDs were synthesized *via* chemical oxidation.^{25, 26} In brief, carbon black
11 (1 g) was added to a mixture of nitric acid_(aq) (100 mL) and DI water (150 mL). The resulting
12 suspension was refluxed for 48 h. The solution was then cooled to room temperature and
13 centrifuged (6000 rpm, 20 min). The supernatant was heated to yield a reddish-brown powder.
14 GQDs were re-dispersed in tetrahydrofuran (THF) and ultra-filtered through a 0.22 μm
15 microporous membrane, resulting in the fluorescent GQDs.
16
17
18
19
20
21
22

23 *Synthesis of bcp-GQDs:* GQDs (0.1 g), trithiocarbonate RAFT agent (0.5 g, 2.1 mmol), DCC
24 (10 mg, 0.05 mmol) and 4-dimethylaminopyridine (DMAP) (1 mg, 0.01 mmol) were mixed in
25 THF overnight at room temperature. Then, the mixture was precipitated into diethyl ether and
26 centrifuged (10000 rpm, 20 min) several times. The resulting material was vacuum-dried, re-
27 dispersed in dimethylformamide (DMF), and filtered through a 0.45 μm PVDF syringe filter.
28 A solution of RAFT-GQDs (100 mg), NIPAAm monomer (0.5 g, 4.4 mmol), and AIBN (6 μmol)
29 in DMF (5 ml) was added into a glass ampoule for polymerization under vacuum. After
30 polymerization for 12 h at 65 $^{\circ}\text{C}$, PNIPAAm-GQDs were precipitated into cold diethyl ether
31 twice and vacuum-dried. A solution of PNIPAAm-GQDs (0.1 g), 7AC monomer (65 mg, 0.23
32 mmol), and AIBN (0.5 mg, 4 μmol) in DMF (5 ml) was added into a glass ampoule for
33 sequential polymerization under vacuum. After reacting for 12 h at 65 $^{\circ}\text{C}$, the product was
34 precipitated in cold diethyl ether twice and vacuum-dried.
35
36
37
38
39
40
41
42
43
44
45
46
47

48 *Characterization:* Detailed procedures are described in the Supporting Information
49
50
51

52 ASSOCIATED CONTENT
53
54

55 **Supporting Information**
56
57
58
59
60

1
2
3
4 Detailed characterization data: TGA, ATR-FTIR, XPS, TEM, SEM, PL spectra, and
5
6 fluorescence decay data. This material is available free of charge via the Internet at
7
8
9 <http://pubs.acs.org>.

11 12 13 14 AUTHOR INFORMATION

15 16 **Corresponding Author**

17
18 *E-mail: bumjoonkim@kaist.ac.kr

19 20 21 22 23 ACKNOWLEDGEMENT

24
25 This work was supported by Samsung Research Funding Center of Samsung Electronics under
26
27 Project Number SRFC-MA1301-07. We thank Rachel Letteri for helpful discussions.
28
29
30
31
32

33 34 35 REFERENCES

- 36 (1) Thomas, S. W.; Joly, G. D.; Swager, T. M., Chemical sensors based on amplifying
37 fluorescent conjugated polymers. *Chem. Rev.* **2007**, *107*, 1339-1386.
38 (2) Medintz, I. L.; Uyeda, H. T.; Goldman, E. R.; Mattoussi, H., Quantum dot
39 bioconjugates for imaging, labelling and sensing. *Nat. Mater.* **2005**, *4*, 435-446.
40 (3) Baldo, M. A.; Thompson, M. E.; Forrest, S. R., High-efficiency fluorescent organic
41 light-emitting devices using a phosphorescent sensitizer. *Nature* **2000**, *403*, 750-753.
42 (4) Schaferling, M., The Art of Fluorescence Imaging with Chemical Sensors. *Angew.*
43 *Chem. Int. Ed.* **2012**, *51*, 3532-3554.
44 (5) Li, C. H.; Zhang, Y. X.; Hu, J. M.; Cheng, J. J.; Liu, S. Y., Reversible Three-State
45 Switching of Multicolor Fluorescence Emission by Multiple Stimuli Modulated FRET
46 Processes within Thermoresponsive Polymeric Micelles. *Angew. Chem. Int. Ed.* **2010**, *49*,
47 5120-5124.
48 (6) Stich, M. I. J.; Fischer, L. H.; Wolfbeis, O. S., Multiple fluorescent chemical sensing
49 and imaging. *Chem. Soc. Rev.* **2010**, *39*, 3102-3114.
50 (7) Yan, X. Z.; Wang, F.; Zheng, B.; Huang, F. H., Stimuli-responsive supramolecular
51 polymeric materials. *Chem. Soc. Rev.* **2012**, *41*, 6042-6065.
52 (8) Hu, J. M.; Liu, S. Y., Responsive Polymers for Detection and Sensing Applications:
53 Current Status and Future Developments. *Macromolecules* **2010**, *43*, 8315-8330.
54 (9) Kim, H. N.; Guo, Z. Q.; Zhu, W. H.; Yoon, J.; Tian, H., Recent progress on polymer-
55 based fluorescent and colorimetric chemosensors. *Chem. Soc. Rev.* **2011**, *40*, 79-93.
56 (10) Pietsch, C.; Hoogenboom, R.; Schubert, U. S., Soluble Polymeric Dual Sensor for
57 Temperature and pH Value. *Angew. Chem. Int. Ed.* **2009**, *48*, 5653-5656.
58
59
60

- 1
2
3
4
5
6
7
8
9
10
11
12
13
14
15
16
17
18
19
20
21
22
23
24
25
26
27
28
29
30
31
32
33
34
35
36
37
38
39
40
41
42
43
44
45
46
47
48
49
50
51
52
53
54
55
56
57
58
59
60
- (11) Paek, K.; Chung, S.; Cho, C. H.; Kim, B. J., Fluorescent and pH-responsive diblock copolymer-coated core-shell CdSe/ZnS particles for a color-displaying, ratiometric pH sensor. *Chem. Commun.* **2011**, 47, 10272-10274.
- (12) Hong, S. W.; Ahn, C. H.; Huh, J.; Jo, W. H., Synthesis of a PEGylated polymeric pH sensor and its pH sensitivity by fluorescence resonance energy transfer. *Macromolecules* **2006**, 39, 7694-7700.
- (13) Yang, H.; Paek, K.; Kim, B. J., Efficient Temperature Sensing Platform Based on Fluorescent Block Copolymer-Functionalized Graphene Oxide. *Nanoscale* **2013**, 5, 5720-5724.
- (14) Hong, S. W.; Kim, D. Y.; Lee, J. U.; Jo, W. H., Synthesis of Polymeric Temperature Sensor Based on Photophysical Property of Fullerene and Thermal Sensitivity of Poly(N-isopropylacrylamide). *Macromolecules* **2009**, 42, 2756-2761.
- (15) Qu, Z. B.; Zhou, X. G.; Gu, L.; Lan, R. M.; Sun, D. D.; Yu, D. J.; Shi, G. Y., Boronic acid functionalized graphene quantum dots as a fluorescent probe for selective and sensitive glucose determination in microdialysate. *Chem. Commun.* **2013**, 49, 9830-9832.
- (16) Yan, X.; Cui, X.; Li, B. S.; Li, L. S., Large, Solution-Processable Graphene Quantum Dots as Light Absorbers for Photovoltaics. *Nano Lett.* **2010**, 10, 1869-1873.
- (17) Ritter, K. A.; Lyding, J. W., The influence of edge structure on the electronic properties of graphene quantum dots and nanoribbons. *Nat. Mater.* **2009**, 8, 235-242.
- (18) Pan, D. Y.; Zhang, J. C.; Li, Z.; Wu, M. H., Hydrothermal Route for Cutting Graphene Sheets into Blue-Luminescent Graphene Quantum Dots. *Adv. Mater.* **2010**, 22, 734-738.
- (19) Zhu, S. J.; Zhang, J. H.; Tang, S. J.; Qiao, C. Y.; Wang, L.; Wang, H. Y.; Liu, X.; Li, B.; Li, Y. F.; Yu, W. L.; Wang, X. F.; Sun, H. C.; Yang, B., Surface Chemistry Routes to Modulate the Photoluminescence of Graphene Quantum Dots: From Fluorescence Mechanism to Up-Conversion Bioimaging Applications. *Adv. Funct. Mater.* **2012**, 22, 4732-4740.
- (20) Shen, J. H.; Zhu, Y. H.; Yang, X. L.; Li, C. Z., Graphene quantum dots: emergent nanolights for bioimaging, sensors, catalysis and photovoltaic devices. *Chem. Commun.* **2012**, 48, 3686-3699.
- (21) Gupta, V.; Chaudhary, N.; Srivastava, R.; Sharma, G. D.; Bhardwaj, R.; Chand, S., Luminescent Graphene Quantum Dots for Organic Photovoltaic Devices. *J. Am. Chem. Soc.* **2011**, 133, 9960-9963.
- (22) Eda, G.; Lin, Y. Y.; Mattevi, C.; Yamaguchi, H.; Chen, H. A.; Chen, I. S.; Chen, C. W.; Chhowalla, M., Blue Photoluminescence from Chemically Derived Graphene Oxide. *Adv. Mater.* **2010**, 22, 505-509.
- (23) Sun, H. J.; Wu, L.; Wei, W. L.; Qu, X. G., Recent advances in graphene quantum dots for sensing. *Mater. Today* **2013**, 16, 433-442.
- (24) Li, L. L.; Wu, G. H.; Yang, G. H.; Peng, J.; Zhao, J. W.; Zhu, J. J., Focusing on luminescent graphene quantum dots: current status and future perspectives. *Nanoscale* **2013**, 5, 4015-4039.
- (25) Yang, H.; Kang, D. J.; Ku, K. H.; Cho, H. H.; Park, C. H.; Lee, J.; Lee, D. C.; Ajayan, P. M.; Kim, B. J., Highly Luminescent Polymer Particles Driven by Thermally Reduced Graphene Quantum Dot Surfactants. *ACS Macro Lett.* **2014**, 3, 985-990.
- (26) Dong, Y. Q.; Chen, C. Q.; Zheng, X. T.; Gao, L. L.; Cui, Z. M.; Yang, H. B.; Guo, C. X.; Chi, Y. W.; Li, C. M., One-step and high yield simultaneous preparation of single- and multi-layer graphene quantum dots from CX-72 carbon black. *J. Mater. Chem.* **2012**, 22, 8764-8766.
- (27) Peng, J.; Gao, W.; Gupta, B. K.; Liu, Z.; Romero-Aburto, R.; Ge, L. H.; Song, L.; Alemany, L. B.; Zhan, X. B.; Gao, G. H.; Vithayathil, S. A.; Kaiparettu, B. A.; Marti, A. A.; Hayashi, T.; Zhu, J. J.; Ajayan, P. M., Graphene Quantum Dots Derived from Carbon Fibers. *Nano Lett.* **2012**, 12, 844-849.

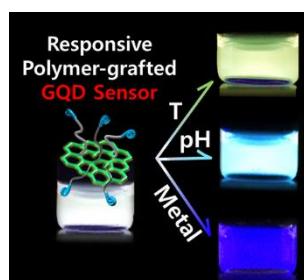
- 1
2
3
4
5 (28) Kwon, W.; Kim, Y. H.; Lee, C. L.; Lee, M.; Choi, H. C.; Lee, T. W.; Rhee, S. W.,
6 Electroluminescence from Graphene Quantum Dots Prepared by Amidative Cutting of Tattered
7 Graphite. *Nano Lett.* **2014**, *14*, 1306-1311.
- 8 (29) Liu, X.; Liu, H. J.; Cheng, F.; Chen, Y., Preparation and characterization of multi
9 stimuli-responsive photoluminescent nanocomposites of graphene quantum dots with
10 hyperbranched polyethylenimine derivatives. *Nanoscale* **2014**, *6*, 7453-7460.
- 11 (30) Dong, Y. Q.; Li, G. L.; Zhou, N. N.; Wang, R. X.; Chi, Y. W.; Chen, G. N., Graphene
12 Quantum Dot as a Green and Facile Sensor for Free Chlorine in Drinking Water. *Anal. Chem.*
13 **2012**, *84*, 8378-8382.
- 14 (31) Hong, C. Y.; You, Y. Z.; Pan, C. Y., Synthesis of water-soluble multiwalled carbon
15 nanotubes with grafted temperature-responsive shells by surface RAFT polymerization. *Chem.*
16 *Mater.* **2005**, *17*, 2247-2254.
- 17 (32) Paek, K.; Yang, H.; Lee, J.; Park, J.; Kim, B. J., Efficient Colorimetric pH Sensor
18 Based on Responsive Polymer-Quantum Dot Integrated Graphene Oxide. *ACS Nano* **2014**, *8*,
19 2848-2856.
- 20 (33) Yoo, M.; Kim, S.; Lim, J.; Kramer, E. J.; Hawker, C. J.; Kim, B. J.; Bang, J., Facile
21 Synthesis of Thermally Stable Core-Shell Gold Nanoparticles via Photo-Cross-Linkable
22 Polymeric Ligands. *Macromolecules* **2010**, *43*, 3570-3575.
- 23 (34) Kwon, T.; Kim, T.; Ali, F. B.; Kang, D. J.; Yoo, M.; Bang, J.; Lee, W.; Kim, B. J.,
24 Size-Controlled Polymer-Coated Nanoparticles as Efficient Compatibilizers for Polymer
25 Blends. *Macromolecules* **2011**, *44*, 9852-9862.
- 26 (35) Nurunnabi, M.; Khatun, Z.; Nafiujjaman, M.; Lee, D. G.; Lee, Y. K., Surface Coating
27 of Graphene Quantum Dots Using Mussel-Inspired Polydopamine for Biomedical Optical
28 Imaging. *ACS Appl. Mater. Interfaces* **2013**, *5*, 8246-8253.
- 29 (36) Deng, Y.; Zhang, J. Z.; Li, Y. J.; Hu, J. H.; Yang, D.; Huang, X. Y., Thermoresponsive
30 graphene oxide-PNIPAM nanocomposites with controllable grafting polymer chains via
31 moderate in situ SET-LRP. *J. Polym. Sci., Part A: Polym. Chem.* **2012**, *50*, 4451-4458.
- 32 (37) Boyer, C.; Liu, J.; Bulmus, V.; Davis, T. P.; Barner-Kowollik, C.; Stenzel, M. H.,
33 Direct synthesis of well-defined heterotelechelic polymers for bioconjugations.
34 *Macromolecules* **2008**, *41*, 5641-5650.
- 35 (38) Yang, Y. F.; Song, X. H.; Yuan, L.; Li, M.; Liu, J. C.; Ji, R. Q.; Zhao, H. Y., Synthesis
36 of PNIPAM Polymer Brushes on Reduced Graphene Oxide Based on Click Chemistry and
37 RAFT Polymerization. *J. Polym. Sci., Part A: Polym. Chem.* **2012**, *50*, 329-337.
- 38 (39) Stuart, M. A. C.; Huck, W. T. S.; Genzer, J.; Muller, M.; Ober, C.; Stamm, M.;
39 Sukhorukov, G. B.; Szleifer, I.; Tsukruk, V. V.; Urban, M.; Winnik, F.; Zauscher, S.; Luzinov,
40 I.; Minko, S., Emerging applications of stimuli-responsive polymer materials. *Nat. Mater.* **2010**,
41 *9*, 101-113.
- 42 (40) Wu, T.; Zou, G.; Hu, J. M.; Liu, S. Y., Fabrication of Photoswitchable and
43 Thermotunable Multicolor Fluorescent Hybrid Silica Nanoparticles Coated with Dye-Labeled
44 Poly(N-isopropylacrylamide) Brushes. *Chem. Mater.* **2009**, *21*, 3788-3798.
- 45 (41) Jares-Erijman, E. A.; Jovin, T. M., FRET imaging. *Nat. Biotechnol.* **2003**, *21*, 1387-
46 1395.
- 47 (42) Clapp, A. R.; Medintz, I. L.; Mauro, J. M.; Fisher, B. R.; Bawendi, M. G.; Mattoussi,
48 H., Fluorescence resonance energy transfer between quantum dot donors and dye-labeled
49 protein acceptors. *J. Am. Chem. Soc.* **2004**, *126*, 301-310.
- 50 (43) Huang, P. J. J.; Liu, J. W., DNA-Length-Dependent Fluorescence Signaling on
51 Graphene Oxide Surface. *Small* **2012**, *8*, 977-983.
- 52
53
54
55
56
57
58
59
60

- 1
2
3
4
5
6
7
8
9
10
11
12
13
14
15
16
17
18
19
20
21
22
23
24
25
26
27
28
29
30
31
32
33
34
35
36
37
38
39
40
41
42
43
44
45
46
47
48
49
50
51
52
53
54
55
56
57
58
59
60
- (44) Clapp, A. R.; Medintz, I. L.; Fisher, B. R.; Anderson, G. P.; Mattoussi, H., Can luminescent quantum dots be efficient energy acceptors with organic dye donors? *J. Am. Chem. Soc.* **2005**, *127*, 1242-1250.
- (45) Medintz, I. L.; Clapp, A. R.; Mattoussi, H.; Goldman, E. R.; Fisher, B.; Mauro, J. M., Self-assembled nanoscale biosensors based on quantum dot FRET donors. *Nat. Mater.* **2003**, *2*, 630-638.
- (46) Dulkeith, E.; Morteaux, A. C.; Niedereichholz, T.; Klar, T. A.; Feldmann, J.; Levi, S. A.; van Veggel, F. C. J. M.; Reinhoudt, D. N.; Moller, M.; Gittins, D. I., Fluorescence quenching of dye molecules near gold nanoparticles: Radiative and nonradiative effects. *Phys. Rev. Lett.* **2002**, *89*, 203002.
- (47) Jones, G.; Jackson, W. R.; Choi, C.; Bergmark, W. R., Solvent Effects on Emission Yield and Lifetime for Coumarin Laser-Dyes - Requirements for a Rotatory Decay Mechanism. *J. Phys. Chem.* **1985**, *89*, 294-300.
- (48) Heyda, J.; Muzdalo, A.; Dzubiella, J., Rationalizing Polymer Swelling and Collapse under Attractive Cosolvent Conditions. *Macromolecules* **2013**, *46*, 1231-1238.
- (49) Xue, C. Y.; Choi, B. C.; Choi, S.; Braun, P. V.; Leckband, D. E., Protein Adsorption Modes Determine Reversible Cell Attachment on Poly(N-isopropyl acrylamide) Brushes. *Adv. Funct. Mater.* **2012**, *22*, 2394-2401.
- (50) Radovic, L. R.; Bockrath, B., On the chemical nature of graphene edges: Origin of stability and potential for magnetism in carbon materials. *J. Am. Chem. Soc.* **2005**, *127*, 5917-5927.
- (51) Yan, X.; Li, Q. Q.; Li, L. S., Formation and Stabilization of Palladium Nanoparticles on Colloidal Graphene Quantum Dots. *J. Am. Chem. Soc.* **2012**, *134*, 16095-16098.
- (52) Ran, X.; Sun, H. J.; Pu, F.; Ren, J. S.; Qu, X. G., Ag Nanoparticle-decorated graphene quantum dots for label-free, rapid and sensitive detection of Ag⁺ and biothiols. *Chem. Commun.* **2013**, *49*, 1079-1081.
- (53) Pasricha, R.; Gupta, S.; Srivastava, A. K., A Facile and Novel Synthesis of Ag-Graphene-Based Nanocomposites. *Small* **2009**, *5*, 2253-2259.
- (54) Liu, Y. Y.; Kim, D. Y., Ultraviolet and blue emitting graphene quantum dots synthesized from carbon nano-onions and their comparison for metal ion sensing. *Chem. Commun.* **2015**, *51*, 4176-4179.
- (55) Ananthanarayanan, A.; Wang, X. W.; Routh, P.; Sana, B.; Lim, S.; Kim, D. H.; Lim, K. H.; Li, J.; Chen, P., Facile Synthesis of Graphene Quantum Dots from 3D Graphene and their Application for Fe³⁺Sensing. *Adv. Funct. Mater.* **2014**, *24*, 3021-3026.
- (56) Mandani, S.; Sharma, B.; Dey, D.; Sarma, T. K., Carbon nanodots as ligand exchange probes in Au@C-dot nanobeacons for fluorescent turn-on detection of biothiols. *Nanoscale* **2015**, *7*, 1802-1808.
- (57) Li, L. L.; Ji, J.; Fei, R.; Wang, C. Z.; Lu, Q.; Zhang, J. R.; Jiang, L. P.; Zhu, J. J., A Facile Microwave Avenue to Electrochemiluminescent Two-Color Graphene Quantum Dots. *Adv. Funct. Mater.* **2012**, *22*, 2971-2979.
- (58) Feng, P.; Zhu, J.; Cheng, Z. P.; Zhang, Z. B.; Zhu, X. L., Reversible addition-fragmentation chain transfer polymerization of 7-(4-(acryloyloxy)butoxy)coumarin. *Polymer* **2007**, *48*, 5859-5866.
- (59) Lim, J.; Yang, H.; Paek, K.; Cho, C. H.; Kim, S.; Bang, J.; Kim, B. J., "Click" Synthesis of Thermally Stable Au Nanoparticles with Highly Grafted Polymer Shell and Control of Their Behavior in Polymer Matrix. *J. Polym. Sci., Part A: Polym. Chem.* **2011**, *49*, 3464-3474.

Table of Contents

Multi-Color Emitting Block Copolymer-Integrated Graphene Quantum Dots for Colorimetric, Simultaneous Sensing of Temperature, pH, and Metal Ions

*Chan Ho Park, Hyunseung Yang, Junhyuk Lee, Han-Hee Cho, Dahin Kim, Doh C. Lee, Bumjoon J. Kim**



*E-mail: bumjoonkim@kaist.ac.kr